Research Article

BIOTECHINTELLECT, 2025, 2 (1) e 11: 1-11
https://jbiotechintel.com/index.php/biotechintel

eISSN: 3115-7920

OPEN ACCESS

Development of Antibody-Imprinted Polymeric Nanomembranes for Rapid and Selective Detection of *Staphylococcus aureus*

Sogand Heydari[1], **Hamed Ahari**[1], **Seyed Amirali Anvar**[2], **Artemiss Mojalal**[2], **Sima Moradi**[3]

[1]*Department of Food Science and Technology, , SR.C., Islamic Azad University, Tehran, Iran*
[2]*Department of Veterinary Hygiene, SR.C., Islamic Azad University, Tehran, Iran*
[3]*Department of Physical Oceanography, , SR.C., Islamic Azad University, Tehran, Iran*

Article history:
Received: 15 Jan 2025
Revised: 18 Feb 2025
Accepted: 25 Mar 2025
Published online: 3 Apr 2025

Keywords:
Staphylococcus aureus detection, Molecularly Imprinted Polymer, nanomembranes, antibody-imprinted polymers, selective bacterial capture, food safety, clinical diagnostic

How to cite this article:
Heydari S, Ahari H, Anvar SA, Mojala A, Moradi S. Development of Antibody-Imprinted Polymeric Nanomembranes for Rapid and Selective Detection of *Staphylococcus aureus*. *BiotechIntellect*. *2025; 2*(1), e11.: 1-11
https://doi.org/10.61882/BiotechIntellect.2.1.24

*corresponding author's email:
hamed_ahari@yahoo.com

ABSTRACT

Identification and isolation of Staphylococcus aureus is of great importance in clinical and food applications, but traditional methods face several drawbacks. Our current investigation focused on developing and evaluating Molecularly Imprinted Polymer (MIP)-functionalized nanomembranes for selective S. aureus capture. MIPs were synthesized on cellulose acetate membranes via UV-initiated polymerization. Characterization via FTIR confirmed antibody integration, while SEM revealed distinct MIP nanoparticles (20-45 nm) compared to larger non-imprinted polymer (NIP) particles (295-2132 nm). Filtration experiments using S. aureus suspensions (10^4-10^5 CFU/mL) demonstrated the membranes' capture capability; notably, filter M3 reduced a 3 × 10^5 CFU/mL challenge concentration to 4.3 × 10^4 CFU/mL in the filtrate. Performance varied across formulations, with differences in filtration times and retention efficiencies observed between MIP and NIP filters. To enhance consistency, further optimization of monomer-to-template ratios is recommended. The MIP filters exhibited robust stability over a two-month evaluation period. These findings highlight the potential of antibody-imprinted MIP nanomembranes as promising tools for S. aureus capture, offering a rapid and selective alternative approach that warrants further optimization and testing in complex matrices for practical applications.

What this article adds:	• Traditional detection methods address challenges with rapid selective detection of *Staphylococcus aureus* in clinical and food safety applications. • The study presents the development of antibody-imprinted polymeric nanomembranes designed for the rapid and selective capture of Staphylococcus aureus.
What this article adds:	• MIPs were synthesized on cellulose acetate membranes through UV-initiated polymerization, resulting in distinct particle sizes that enhance the specificity and efficiency of bacterial capture compared to non-imprinted polymers. • Results demonstrated effective filtration capabilities, with MIP filters significantly reducing the concentration of S. aureus in suspensions, showcasing their potential as efficient tools for the detection of this pathogen. • The study highlights the robust stability of the MIP filters over a two-month period and suggests further optimization of the monomer-to-template ratios to enhance filtration efficiency and consistency. • The findings underscore the potential application of MIP nanomembranes in food safety and clinical diagnostics, prompting further research to validate their performance in complex matrices and explore alternative templates for improved binding site access.

1. Introduction

The effective detection and monitoring of pathogenic microorganisms remain a critical challenge across various sectors, including clinical diagnostics, environmental surveillance, and particularly, food safety. Among the prominent foodborne pathogens, *Staphylococcus aureus* is considered one of the most persistent food-contaminated pathogens due to its production of heat-resistant enterotoxins, and methicillin-resistant strains of this bacterium (MRSA) must be detected by rapid, accurate, and precise methods [1].

Traditional methods for bacterial detection, such as standard microbiological culturing, while considered the gold standard, are often difficult, time-consuming (requiring 24-72 h), and may lack the necessary selectivity in complex matrices [2]. While genetic based procedures like Polymerase Chain Reaction (PCR) offer higher sensitivity and speed, they typically require sophisticated equipment, trained personnel, and extensive sample pre-treatment, limiting their applicability for routine laboratory analysis. Immunoassays, relying on antibody-antigen interactions, can provide selectivity but may suffer from limitations related to antibody stability, production costs, and potential cross-reactivity [3].

To overcome these limitations, significant research effort has been directed towards developing alternative recognition elements and sensing platforms. Nanotechnology, in particular, offers promising opportunities through substances characterized by extensive surface area relative to their volume and distinct physical and chemical attributes. Within this domain, Molecularly Imprinted Polymers (MIPs) have emerged as a compelling group of artificial materials crafted to replicate the specific binding functionalities of biological molecules such as antibodies and enzymes. [4, 5].

These materials are crafted by polymerizing functional and cross-linking monomers in the presence of a template molecule (or microorganism). Once the polymerization process is complete, the template is extracted, resulting in cavities within the polymer matrix that are tailored for specific recognition, based on their precise dimensions, structural features, and chemical properties [6]. The process of "molecular imprinting" facilitates the development of durable and affordable synthetic receptors, which exhibit exceptional affinity and specificity towards target analytes. These targets can range from small molecules and large biomolecules to entire cells, such as bacteria. Compared to their biological counterparts, MIPs generally offer superior stability under harsh environmental conditions (pH, temperature) and longer shelf-life [7].

Integrating MIP technology with separation or sensing platforms, such as membranes or filters, holds potential for developing simple yet effective tools for bacterial capture and detection. An MIP-based filter could selectively trap target bacteria from a sample matrix, facilitating downstream detection or quantification, or even acting as a preliminary sample concentration step. This study aimed at development and evaluation of nanomembranes functionalized with MIPs specifically designed for the selective capture of *Staphylococcus aureus*. Future studies should explore alternative templates, such as surface proteins, to enhance binding site accessibility.

2. Materials and Methods

2.1. Chemicals and Reagents

All the chemicals and reagents utilized in this investigation were of analytical grade and, unless specified otherwise, obtained from Sigma-Aldrich (St. Louis, MO, USA). The anti-*Staphylococcus aureus* antibody, conjugated with horseradish peroxidase (HRP, ab156662), was acquired in pre-packaged commercial form from a local supplier in Tehran, Iran. Cellulose acetate (CA) membranes (Gyrodisk, Orange

Scientific, Sartorius, Switzerland), were utilized as the foundation for filter (1.2 µm pore size) synthesis. The bacterial strain *Staphylococcus aureus* (PTCC 1431) was obtained from the Pasterur Inistitute of Iran, Tehran. Brain Heart Infusion (BHI, HiMedia) broth and Baird-Parker agar (HiMedia, India) were prepared for *S.aureus* cultivation and enumeration. The synthesis of the MIP employed methacrylic acid (MAA) as the functional monomer, ethylene glycol dimethacrylate (EGDMA) as the crosslinking agent, and azobisisobutyronitrile (AIBN) as the polymerization initiator, with their respective molecular weights being 86.09 g/mol, 198.22 g/mol, and 164.21 g/mol. Additional reagents included acetic acid, phosphate buffer saline (PBS), acetate buffer, peptone water (diluted 1:1000), physiological saline (0.9% NaCl), methanol, deionized water for synthesis, and double-distilled water for experimental procedures.

2.2. Equipment

The experimental procedures relied on a suite of specialized instruments to ensure accuracy and consistency. A pH meter (GLP, Digital pH meter) facilitated buffer preparation and pH adjustments. Bacterial growth was tracked using a spectrophotometer (Shimadzo, Japan), and an incubator maintained at 37°C provided optimal conditions for culturing. Heat treatments were conducted in a water bath, while a centrifuge (Model 5810, Eppendorf) enabled bacterial harvesting and washing. An autoclave ensured sterilization of materials, and a vacuum filtration system (Millipore) was employed for filtration experiments. MIP synthesis utilized a UV irradiation device (CAMAG UV lamp, 254 nm) to initiate polymerization, complemented by a sonicator (Fritsch, Germany) for degassing and filter maintenance. The morphology of the filter was examined using a Scanning Electron Microscope (SEM, Zeiss, Germany) to assess its structural features and surface characteristics and a vacuum funnel supported washing and bacterial capture processes.

2.3. Synthesis of Filters

In the first step, the synthesis of MIP and NIP filters was performed on cellulose acetate (CA) membranes using a UV-initiated radical polymerization technique, adapted from previous studies [8]. Initially, CA membranes were trimmed to appropriate sizes and cleaned with deionized water to eliminate contaminants. For MIP preparation, the membranes were submerged in a polymerization mixture comprising MAA (0.086–0.344 mL), EGDMA (2.6 mL, 14 mmol), AIBN (120–214.3 mg), and the anti-*S. aureus* antibody as the template, all dissolved in a buffered solution. NIP filters, designed as controls to assess non-specific binding, were made using the same method but omitted the antibody template. Five MIP filters (MIP1–MIP5) and five NIP filters (NIP1–NIP5) were produced, with MAA quantities adjusted to optimize the monomer-to-template ratio, while EGDMA and AIBN remained consistent across most formulations (Table 1).

The polymerization mixture was degassed using a sonicator (Fritsch, Germany) at 25°C for 10 minutes to remove dissolved gases, followed by a 3-minute purge with nitrogen gas (Roham Gas,N_2, 99.999% purity) to exclude oxygen, which could hinder polymerization. The degassed solution was then placed in a UV chamber (CAMAG) and exposed to 254 nm irradiation for 20 hours at room temperature, triggering radical polymerization and forming polymer particles on the CA membrane fibers. Post-polymerization, the filters were rinsed with 500 mL of a methanol and acetic acid solution prepared in a 95:5 volume ratio to extract the antibody template from MIP filters and remove unreacted monomers from both MIP and NIP filters. To enhance cleaning efficiency, the filters underwent sonication in the washing solution for 10–15 minutes, and then rinsed with deionized water. Filters were stored hydrated to maintain structural integrity.

Table 1. Composition of MIP and NIP Filters synthetized in this study

Filter	MAA (mL)	EGDMA (mL)	AIBN (mg)	Template (Antibody)
MIP1	0.086	2.6	120	Yes
MIP2	0.124	2.6	214.3	Yes
MIP3	0.172	2.6	214.3	Yes
MIP4	0.258	2.6	214.3	Yes
MIP5	0.344	2.6	214.3	Yes
NIP1	0.086	2.6	214.3	No
NIP2	0.124	2.6	214.3	No
NIP3	0.172	2.6	214.3	No
NIP4	0.258	2.6	214.3	No
NIP5	0.344	2.6	214.3	No

2.4. Preparation of Bacterial Suspension

The *S. aureus* strain PTCC 1431 was cultivated in in BHI broth at 37°C for overnight, in accordance with Iranian Standard No. 1-6806. Then, grown bacteria were harvested via centrifugation at 3300 rpm for 9 minutes and rinsed with physiological saline (0.9% NaCl) to eliminate media residues. The collected suspension underwent heat treatment by being placed in a boiling water bath for 20 minutes to neutralize capsular polysaccharides that might affect detection. The turbidity of the bacterial suspension was standardized to approximately 1 × 10^8 CFU/mL using a spectrophotometer. Serial dilutions in peptone water at a 1:1000 ratio were then performed to achieve different concentrations. Then, 10^5 CFU/mL concentration was chosen for primary testing, reflecting the pathogenicity threshold for *S. aureus*.

2.5. Filtration Experiments and Bacterial Capture

Filtration experiments were conducted using a Millipore filtration system, with each filter (MIP1–MIP5, NIP1–NIP5, and a raw CA control) positioned on the support disk. Filters were pre-wetted with sterile distilled water to ensure uniform flow and prevent creasing. A 25 mL aliquot of *S. aureus* suspension (10^4 or 10^5 CFU/mL) was filtered through each unit, with a vacuum pump maintaining a pressure of 10 kPa and flow rates between 0.1 and 0.4 mL/min to optimize bacterial contact time. Filtrates were collected in sterile containers for analysis. For enumeration, 0.1 mL of filtrate was plated in triplicate on BP agar and kept at 37°C for overnight, followed by colony counting to determine the number of bacteria passing through. Capture efficiency was assessed by comparing filtrate counts from MIP filters to those from NIP filters and the CA control. Sensitivity was further tested using 10^1 to 10^8 CFU/mL suspensions.

2.6. Antibody Elution and pH Optimization

Antibody elution experiments verified template removal and binding site functionality in MIP filters. Filters were exposed to varying anti-*S. aureus* antibody doses, captured via a vacuum funnel, and eluted with dilute acetic acid. The optimal elution pH was determined by testing phosphate and acetate buffers from pH 5.5 to 8.5, monitored with a pH meter. Eluate antibody concentrations were quantified using a diagnostic kit, and the pH yielding the highest recovery was selected, calculated as:

% Recovery = (Ab concentration in eluate – Initial Ab concentration/Initial Ab concentration)×100

This process confirmed the MIP filters' ability to release the template, ensuring functional binding sites for bacterial capture.

2.7. Filter Washing and Maintenance

Post-filtration, filters were cleaned to remove trapped bacteria or residual antibody. Each filter was washed in a vacuum funnel with 50 mL of a mixture of methanol and acetic acid solution (95:5 by volume), followed by sonication for 12 minutes to clear clogged pores and residual particles. Filters were then rinsed with deionized water and stored in distilled water to maintain hydration and prevent structural damage.

2.8. Flow Rate Determination

The optimal filtration flow rate was established by passing 50 mL of peptone water through a raw CA

filter. Without vacuum, this took approximately 8 minutes (6 mL/min); with minimal vacuum, it reduced to 30 seconds. In addition, flow rate (6 mL/min) without vacuum was selected to balance contact time and filter integrity for all subsequent experiments.

2.9. Filter Characterization

Filter morphology was assessed via scanning electron microscopy in Engineering Laboratory, Islamic Azad University, Science and Research Branch. Filter sections were mounted on stubs, gold-coated for 10 minutes using a sputter coater and imaged at 2500× and 5000× magnifications to examine surface structure and polymer particle presence. For particle size analysis, filters were immersed in acetonitrile, pressed between glass slides, dried under nitrogen, gold-coated, and imaged at 10× magnification to evaluate particle size and distribution.

2.10. Sensitivity and Shelf-Life Evaluation

The sensitivity of the optimal MIP filter was tested with bacterial suspensions from 10^1 to 10^8 CFU/mL, with filtrates plated on Baird-Parker agar to determine the lowest detectable concentration. Shelf life was evaluated over two months, with capture efficiency tested every four days using a 10^5 CFU/mL suspension, assessing filter stability under standard storage conditions.

2.11. Statistical Analysis

To ensure reliability, all experiments were conducted in sets of three. Bacterial counts were analyzed using SPSS 21 and Excel 2010, with statistical differences between MIP and NIP filters evaluated via t-tests or ANOVA, setting significance at p value below 0.05.

3. Results and Discussion

3.1 Optimized Parameters

3.1.1 Suitable Solvent

The selection of an appropriate solvent was fundamental in this study. Among the evaluated options—water, chloroform, acetonitrile, and their mixtures—a combination of acetonitrile and water at a 20:80 (v/v) ratio proved optimal. This solvent mixture successfully dissolved the target analyte, functional monomer, crosslinker, and initiator after 2 minutes of sonication, while exhibiting no chemical interactions with these components, thereby ensuring efficient polymer formation.

3.1.2 Selection of Initiator

The initiator concentration significantly influenced the polymerization process. An optimal amount of 1.5 mmol was identified, as lower concentrations failed to initiate the reaction, and higher amounts, coupled with increased functional monomer levels, reduced polymer yield. This concentration enabled the successful preparation of loaded membranes.

3.2 Structural and Property Analysis of the Synthesized Molecularly Imprinted Polymer

3.2.1 FTIR Analysis

FTIR spectra of MIP and NIP samples revealed distinct structural features (Figure 1). A broad peak between 3100 and 3700 cm^{-1} indicated O-H stretching vibrations from hydroxyl groups. The peaks observed at 2940 and 2880 cm^{-1} corresponded to asymmetric and symmetric C-H stretching, in that order. A sharp peak at 1737 cm^{-1} was attributed to C=O stretching in methacrylic acid and cellulose acetate, while a smaller peak at 1647 cm^{-1} suggested aromatic cycle structure. An additional peak at 1431 cm^{-1} was linked to asymmetric C-O stretching in COOH groups. Another peak at 1369 cm^{-1} was associated with C-H bending in CH_3 groups. Peaks at 1220, 1161, and 1032 cm^{-1} were associated with carbon and oxygen bands stretching vibrations, respectively, while peaks at 901 and 605 cm^{-1} indicated C-H rocking and out-of-plane vibrations in aromatic rings. Upon antibody incorporation into the MIP, increased intensities were observed for peaks related to hydroxyl (3500 and 1647

cm^{-1}), carbonyl (1737 cm^{-1}), and CH_3 (1369 cm^{-1}) groups. A marked intensity increase at 688 cm^{-1} in the MIP sample suggested the addition of aromatic rings from the antibody. Shifts of 5–20 cm^{-1} in hydrogen-containing group peaks further indicated hydrogen bonding between the composite and the antibody, confirming its successful integration.

3.2.2 Electron Microscopy Observations

SEM images demonstrated that MIP particle sizes ranged from 20 to 45 nm, while NIP particles were larger, between 295 and 2132 nm (Figure 2). Higher functional monomer concentrations reduced particle sizes below 100 nm. The images confirmed effective loading of MIP particles into membrane pores, with smaller particle sizes in MIP filters attributed to the presence of the template molecule, unlike NIP filters. Dark aggregates observed were due to incomplete dissolution in acetonitrile.

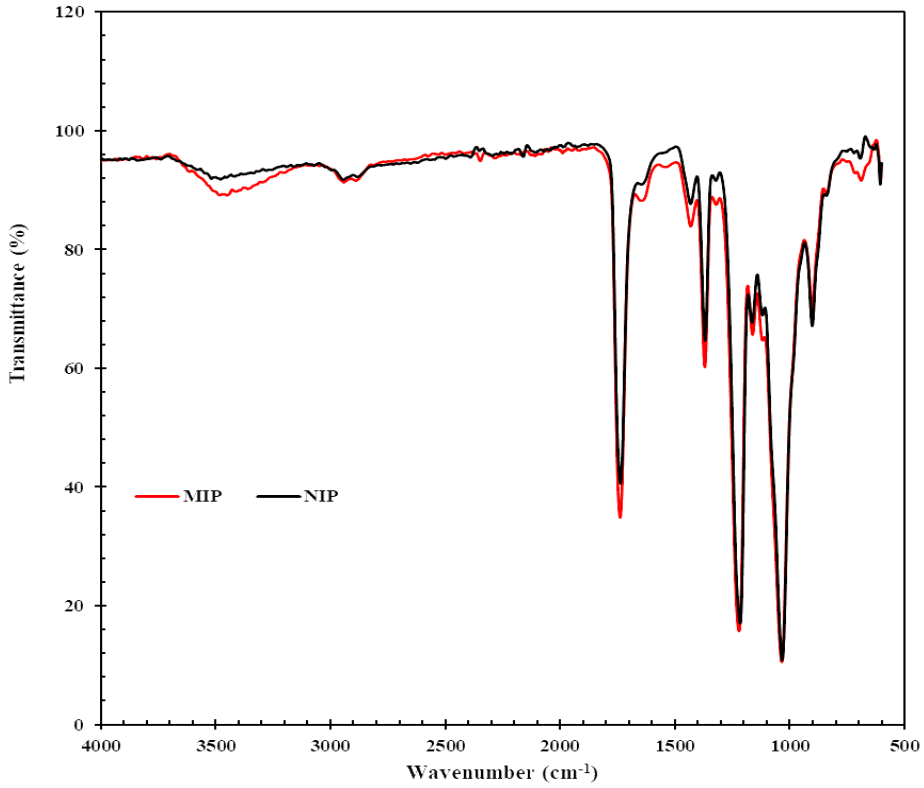

Figure 1: FTIR analysis of the synthetised MIP and NIP samples.

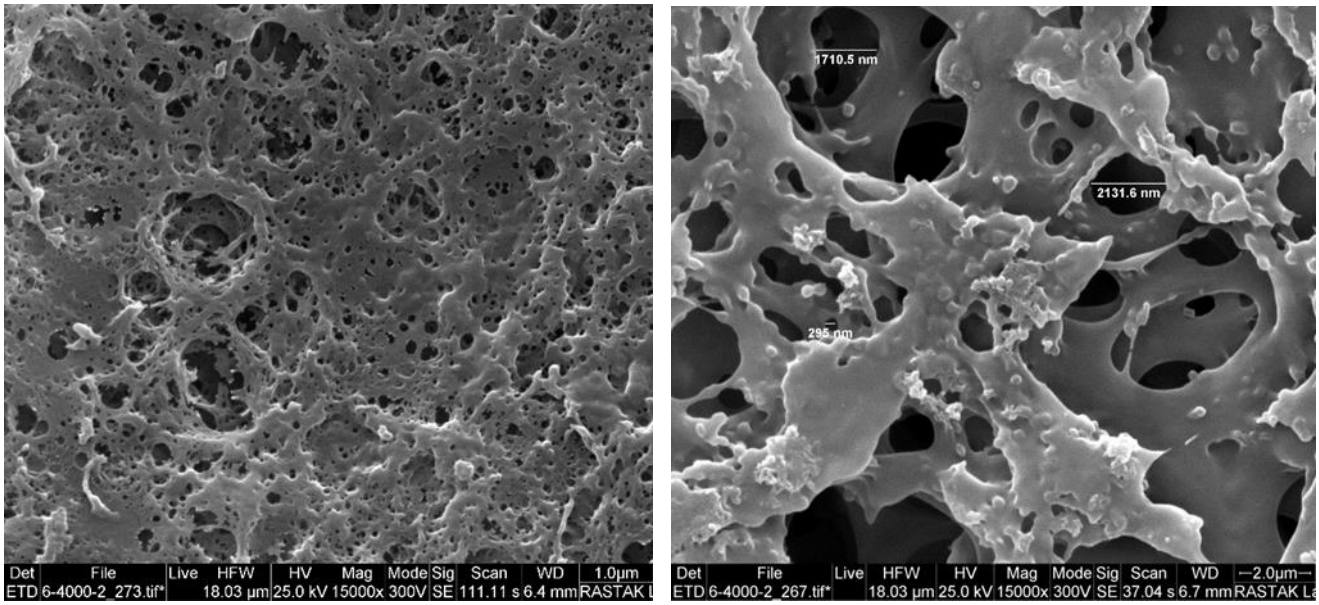

Figure 2: Microscopic image of molecularly imprinted polymer. Left) at KX 15 magnification with a particle diameter of 1 µm, right) at KX 15 magnification with a particle diameter of 2 µm

3.3 Membrane (Filter) Behavior

3.3.1 Washing Performance

Filter washing behavior varied across samples. For filter N2 (NIP2), 20 mL of washing solution required 12 minutes to pass, while N3 processed 50 mL in 14 minutes, and N4 handled 20 mL in 7 minutes. Filter N5 exhibited blockage, preventing solution passage. Filters M1 (MIP1), M2, and M3 also showed no flow with 20 mL, whereas M4 and M5 processed 20 mL in 4 and 2 minutes, respectively (Table 2).

Table 2: Membrane (Filter) Washing Behavior

Filter Number	Filtration Volume (mL)	Time (min)
N2	20	12
N3	20	14
N4	20	7
N5	20	-
M4	20	4
M5	20	2

3.3.2 Microbial Suspension Filtration

The filtration process for microbial suspensions was designed to achieve an optimal balance between sufficient contact time for effective absorption by the filters and the prevention of structural damage due to excessive duration. Consequently, it was determined that a vacuum pump would not be employed for the baseline washing procedure. Instead, a flow rate of 6 mL/s was established, allowing 50 mL of washing solution or culture medium to pass through each filter in approximately 8 minutes. To accommodate the washing of ten filters—five MIP (MIP5) and five NIP (NIP5)—a total of 500 mL of washing solution was prepared. However, during microbial filtration experiments, a vacuum pump was utilized at its minimal pressure setting to facilitate controlled passage of the suspension.

The behavior of the filters during microbial suspension filtration varied significantly across the samples tested with 25 mL of a microbial suspension. For filter N2, the passage of the suspension required 20 minutes, indicating a relatively slow filtration rate. Filter N3 exhibited an even longer duration, taking 23 minutes for the same volume to pass through, suggesting potential differences in pore structure or surface interactions. In contrast, filter N4 demonstrated a more moderate filtration time of 17 minutes, reflecting a balanced performance. Among the MIP filters, M4

displayed exceptional efficiency, processing the 25 mL suspension in just 2 minutes, which may indicate a highly accessible pore network or reduced resistance to flow. Filter M5, while still efficient relative to the NIP filters, required 12 minutes for the same volume, suggesting a moderate capacity for microbial retention and flow.

These filtration times highlight distinct performance profiles among the filters, with MIP filters generally outperforming their NIP counterparts in terms of speed, likely due to the templated structure enhancing flow dynamics or microbial capture efficiency. The observed variations underscore the influence of polymer composition and imprinting on filtration behavior, providing valuable insights into the practical application of these membranes for microbial separation tasks.

3.3.3 Bacterial Retention Efficiency

After passing a 10^4 CFU/mL microbial suspension through the filters, bacterial counts in the filtrate varied. Filter N3 exhibited the highest retention (1 CFU/mL), while M4 showed the lowest (1.2×10^4 CFU/mL). Other results included N2 (1.1×10^2 CFU/mL), N4 (2.4×10^2 CFU/mL), and M5 (1.1×10^2 CFU/mL). Using a 3×10^5 CFU/mL suspension with 15 mL filtered at 25 mmHg, filtration times ranged from 1:24 minutes (NULL filter) to 13:55 minutes (M3). Filter N4 showed the lowest bacterial count in the filtrate (1×10^2 CFU/mL), while N5 had the highest (3×10^5 CFU/mL). Filter M3, with the longest filtration time, retained significant bacteria (filtrate: 4.3×10^4 CFU/mL) (Figure 3).

The threat of *S. aureus* in food production and healthcare requires the development of rapid, selective, and robust detection methods beyond conventional culturing or complex molecular techniques. Here we explored the fabrication and application of MIP-functionalized nanomembranes specifically designed for S. aureus capture, leveraging the advantages of molecular imprinting technology.

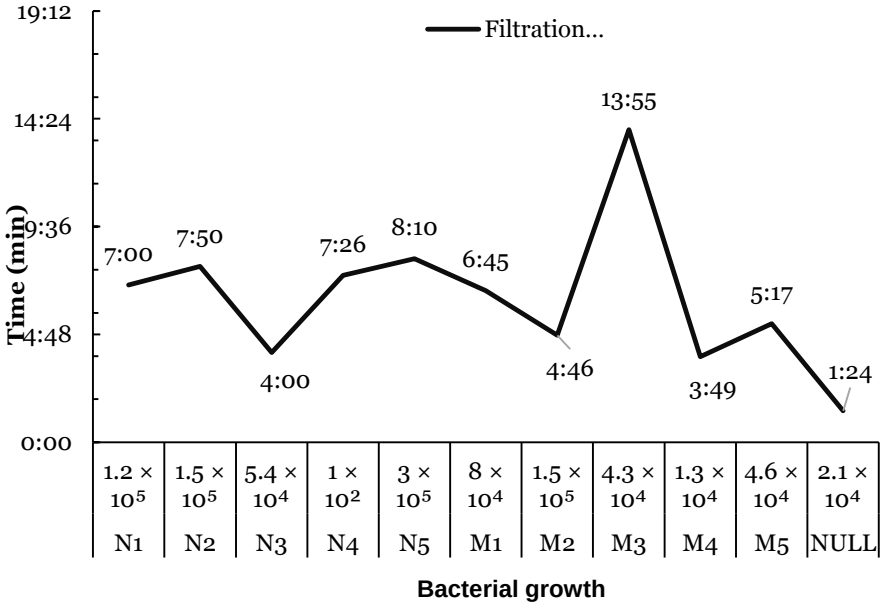

Figure 3: Results of the Filtration Time and Bacterial Growth at 25 mmHg.

A key aspect of this work was the use of an anti-S. aureus antibody as the biological template during the polymerization of MAA and EGDMA. This method aims to create highly specific recognition sites mimicking the antibody's binding paratope. While theoretically promising for selectivity, using large,

complex biomolecules like antibodies as templates can present challenges, including potential conformational changes during polymerization or incomplete template removal, which might affect the fidelity and accessibility of binding sites [9]. To address this, future studies could explore alternative templates, such as surface proteins or whole bacterial cells, to improve binding site functionality. Nevertheless, the characterization data (FTIR, SEM) suggested successful imprinting occurred, leading to distinct morphological features, notably the formation of MIP nanoparticles (20-45 nm) significantly smaller than the NIP control particles (295-2132 nm). This size difference is consistent with template-influenced polymer growth. The chosen MAA/EGDMA system is well-established for creating MIPs, often yielding effective recognition for various analytes, including bacteria [10,11].

The functional evaluation focused on filtration performance and bacterial retention. Filtration times varied significantly among formulations, with MIP filters M4 (6 min) and M5 (12 min) processing microbial suspensions faster than some NIP counterparts, suggesting the imprinted cavities might favorably influence flow dynamics or accelerate capture. Bacterial retention efficiency, assessed by analyzing filtrate counts, demonstrated the filters' ability to capture *S. aureus*. For example, when challenged with a 3×10^5 CFU/mL suspension, filter M3 yielded a filtrate count of 4.3×10^4 CFU/mL, indicating substantial bacterial removal, although it exhibited the longest filtration time (13:55 min). This performance is comparable to Doostmohammadi et al [12] and Chen et al [13] studies using MIP membranes for bacteria removal. Interestingly, the NIP filter N4 also showed high retention in one experiment (filtrate count 1×10^2 CFU/mL from 10^4 CFU/mL challenge), highlighting that physical factors like pore size and non-specific adsorption contribute to bacterial capture alongside specific MIP binding sites, a phenomenon also observed in standard filter testing [14]. Standardized tests, such as those following ASTM protocols, often report efficiencies exceeding 99.9% under specific challenge conditions [15], and future studies should adopt matched protocols for direct comparison with commercial filters.

A significant advantage of MIPs over biological receptors is their enhanced stability and potential for reusability [16,17]. This study noted robust stability over 32 days, consistent with the known robustness of these synthetic polymers. While reusability cycles were not performed, future investigations should include regeneration tests to assess the filters' potential for multiple uses, enhancing cost-effectiveness [18].

However, the observed variability in filtration times and the potential for filter blockage indicate that optimizing the interplay between specific binding, non-specific interactions, and membrane permeability is crucial. Future investigations should focus on refining monomer/crosslinker ratios and pore structure to enhance both selectivity and flow rate, as well as testing in complex matrices like food samples to validate real-world applicability [19]. Integrating these MIP filters with a rapid detection modality could further advance their utility for point-of-need diagnostics or inline monitoring in industrial settings.

4. Conclusion

In conclusion, this work contributes to the growing field of MIP-based bacterial recognition by demonstrating the fabrication of antibody-imprinted nanomembranes capable of capturing S. aureus. The results highlight the potential of MIP filters as stable and selective tools, while also pointing towards areas for further optimization, including reusability testing and validation in complex matrices, to bridge the gap towards practical, high-performance applications in food safety and diagnostics.

5. Declarations

5.1. Acknowledgments

The authors are thankful to the Islamic Azad University, Science and RsearchBranch for their partial support of this work.

5.2. Authors' Contributions

All authors equally contributed to this work.

5.3. Declaration of Interest

The authors of this article declared no conflict of interest.

5.4. Ethical Considerations

All ethical principles were adhered in conducting and writing this article.

5.5. Transparency of Data

In accordance with the principles of transparency and open research, we declare that all data and materials used in this study are available upon request.

5.6. Funding

This research was carried out independently with personal funding and without the financial support of any governmental or private institution or organization.

5.7. Using Artificial Intelligent chatbots

No AI chatbot has been used in this study.

References

1. Rubab M, Shahbaz HM, Olaimat AN, Oh D-H. Biosensors for rapid and sensitive detection of Staphylococcus aureus in food. Biosensors and Bioelectronics. 2018;105:49-57.
2. Chang Y-C, Yang C-Y, Sun R-L, Cheng Y-F, Kao W-C, Yang P-C. Rapid single cell detection of Staphylococcus aureus by aptamer-conjugated gold nanoparticles. Scientific reports. 2013;3(1):1863.
3. Suaifan GA, Alhogail S, Zourob M. Rapid and low-cost biosensor for the detection of Staphylococcus aureus. Biosensors and Bioelectronics. 2017;90:230-7.
4. Xu X, Lin X, Wang L, Ma Y, Sun T, Bian X. A novel dual bacteria-imprinted polymer sensor for highly selective and rapid detection of pathogenic bacteria. Biosensors. 2023;13(9):868.
5. Zhang J, Wang Y, Lu X. Molecular imprinting technology for sensing foodborne pathogenic bacteria. Analytical and bioanalytical chemistry. 2021;413(18):4581-98.
6. Wang R, Wang L, Yan J, Luan D, Wu J, Bian X. Rapid, sensitive and label-free detection of pathogenic bacteria using a bacteria-imprinted conducting polymer film-based electrochemical sensor. Talanta. 2021;226:122135.
7. Allender CJ, Richardson C, Woodhouse B, Heard CM, Brain KR. Pharmaceutical applications for molecularly imprinted polymers. International journal of pharmaceutics. 2000;195(1-2):39-43.
8. BelBruno JJ. Molecularly imprinted polymers. Chemical reviews. 2018;119(1):94-119.
9. Agar M, Laabei M, Leese HS, Estrela P. Multi-Template Molecularly Imprinted Polymeric Electrochemical Biosensors. Chemosensors. 2025;13(1):11.
10. Vahid S, Ahari H, Adergani BA, Reihani SFS. Designing a molecularly imprinted polymer-based nanomembrane for the selective removal of Staphylococcus aureus from aqueous media. Applied Food Biotechnology. 2021;8(4):275-84.
11. Elhabal SF, Abdelmonem R, El Nashar RM, Elrefai MFM, Hamdan AME, Safwat NA, et al. Enhanced antibacterial activity of clindamycin using molecularly imprinted polymer nanoparticles loaded with polyurethane nanofibrous scaffolds for the treatment of acne vulgaris. Pharmaceutics. 2024;16(7):947.
12. Doostmohammadi A, Youssef K, Akhtarian S, Tabesh E, Kraft G, Brar SK, et al. Molecularly imprinted polymer (MIP) based core-shell microspheres for bacteria isolation. Polymer. 2022;251:124917.
13. Chen M, Lu J, Gao J, Yu C, Xing W, Dai J, et al. Design of self-cleaning molecularly imprinted membrane with antibacterial ability for high-selectively separation of ribavirin. Journal of Membrane Science. 2022;642:119994.
14. Whyte HE, Montigaud Y, Audoux E, Verhoeven P, Prier A, Leclerc L, et al. Comparison of bacterial filtration efficiency vs. particle filtration efficiency to assess the performance of non-medical face masks. Scientific Reports. 2022;12(1):1188.

15. Tse Sum Bui B, Auroy T, Haupt K. Fighting Antibiotic-Resistant Bacteria: Promising Strategies Orchestrated by Molecularly Imprinted Polymers. Angewandte Chemie International Edition. 2022;61(8):e202106493.
16. Idil N, Mattiasson B. Imprinting of microorganisms for biosensor applications. Sensors. 2017;17(4):708.
17. Gkika DA, Tolkou AK, Lambropoulou DA, Bikiaris DN, Kokkinos P, Kalavrouziotis IK, et al. Application of molecularly imprinted polymers (MIPs) as environmental separation tools. RSC Applied Polymers. 2024;2(2):127-48.
18. Liedtke C, Bienge K, Wiesen K, Teubler J, Greiff K, Lettenmeier M, et al. Resource use in the production and consumption system—The MIPS approach. Resources. 2014;3(3):544-74.
19. Li G, Row KH. Recent applications of molecularly imprinted polymers (MIPs) on micro-extraction techniques. Separation & Purification Reviews. 2018;47(1):1-18.